Axial load effects on flush end-plate moment connections

Alireza Goudarzi MSc
PhD Student, Department of Civil Engineering, Amirkabir University of Technology, Tehran, Iran

Mehdi Ghassemieh PhD
Professor, School of Civil Engineering, University of Tehran, Tehran, Iran

Nader Fanaie PhD
Assistant Professor, Department of Civil Engineering, K. N. Toosi University of Technology, Tehran, Iran

Debra Fern Laefer PhD
Professor, Urban Modelling Group, School of Civil Engineering and the Earth Institute, University College Dublin, Dublin, Ireland (corresponding author: debra@laefer.com)

Mahmoud Baei MSc
Researcher, School of Civil Engineering, University of Tehran, Tehran, Iran

This numerical study focuses on the behavior of flush, end-plate, moment connections subjected to combined bending moment and axial force. Beams within frames are subjected to lateral loads (e.g. earthquake and wind) in the form of axial forces and bending moments. Thus, both must be considered in seismic design. In pitched-roof portal frames, sway frames or frames with incomplete floors, the level of axial forces in such joints may be significant. To partially fulfill this dual requirement, two distinctive flush, end-plate, moment connections were investigated: one to exhibit thick, connection-plate behavior and the other to exhibit thin, connection-plate behavior. The magnitude of the imposed axial force changes the failure mode. When subjected to reversed cyclic loading, distinctive behaviors between the two end-plate connection types were observed. During cyclic loading, in the axial compressive force phase, there was an increase in the ultimate bending moment, yielding bending moment, initial stiffness, and dissipated energy. Reductions occurred in all of these elements during the tensile axial force phase. As expected, the thin end-plate had notably higher ductility than the thick end-plate connection. In both connections, the maximum moment capacity under compressive axial force nearly equaled 30% of the beam's section yield stress.

Notation

$F_{\text{y-beam}}$	beam yield stress
M_{np}	bolts' moment without the prying force (kNm)
M_{pl}	plastic moment of end-plate (kNm)
$M_{\text{u-FE}}$	ultimate moment capacity of connection from finite-element modelling (kNm)
P	axial stress applied to beam section
R	ultimate moment ratio of connection with axial load to without axial load
ϕ	joint rotation

1. Introduction

Flexural connections with a flush end-plate are composed of a connecting plate welded to the end of a beam that is then bolted to a column or second beam segment by using several rows of high-strength bolts. End-plate moment connections can be categorised as flush end-plate or extended end-plate. In the flush group, the end-plate height does not exceed the edges of the beam flanges, and all connecting bolts appear in the area between the two beam flanges (Figure 1). This type of connection is commonly used in frames with short beams subjected to standard gravitational loads and only small lateral loads. The flush end-plate connection can be configured with or without a stiffener. In the stiffened arrangement, the stiffeners are welded to the beam's web, and the end-plates are placed between or outside the connecting bolt rows. Figures 1 and 2 show four different configurations of the flush end-plate connection that are normally used as beam-to-column connectors.

The second type is composed of an end-plate whose height extends beyond the beam flanges and has at least one row of bolts in the extended part of the end-plate. This extended end-plate can be used with or without stiffeners, which is connected by a weld to the outside of the beam flange and the end-plate. The stiffeners are aligned with the beam's web to stiffen the extended part of the end-plate and to reduce the end-plate's required thickness. Figure 3 shows two extended, end-plate moment connections. These types are normally used in heavier steel frames.

When the connections are subjected to gravitational loading or wind-type lateral loading, they are often designed to transfer only the tensile force of the beam flange, which may necessitate the application of additional bolt rows around the tensile flange of the beam. In seismic loading, however, the connecting end-plates are designed for the tensile forces of both flanges of the beam. In this case, the connection must be designed so that a plastic hinge can form in the beam at a proper distance from the column face. This conforms to the 'strong column/weak beam' design criterion (ANSI/AISC 341-05 (ANSI/AISC, 2005a)).

2. Background

Considerable studies have been undertaken on the behaviour of bolted connections. These can be classified as experimental, analytical or numerical, but more commonly are a combination of these. Early experimental work was done by Bose *et al.* (1997) using both full-scale experiments and
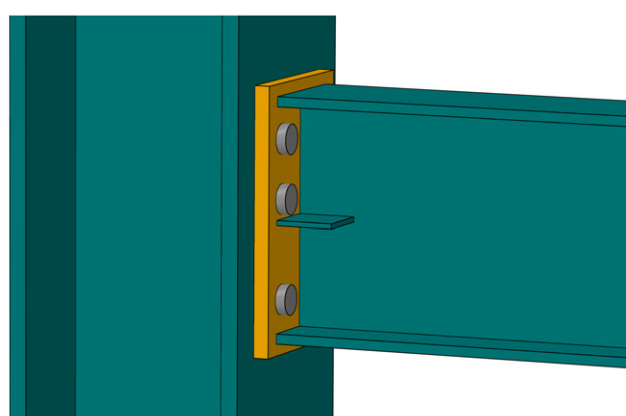
Figure 1. Unstiffened flush end-plate moment connection: (a) two bolts; (b) four bolts
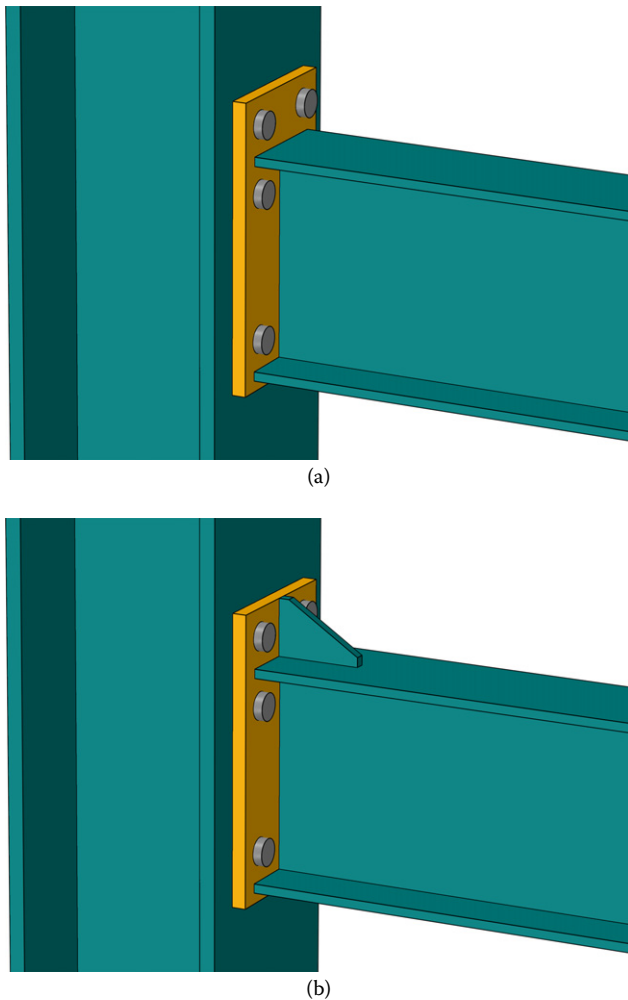

Figure 2. Flush end-plate moment connection with stiffener: (a) four bolts with stiffener between the bolts; (b) four bolts with stiffener outside the bolts

finite-element modelling to investigate unstiffened, flush end-plate connections with two and four bolts. Soon after, Boorse (1999) investigated the inelastic rotation capability of flush end-plate moment connections. The inelastic rotation of fully restrained connections in a steel moment frame during an earthquake is used to dissipate the energy added to the structural system by seismic loading. The inelastic rotation of the connections was calculated and conclusions were drawn, as to the compliance of these connections with American Institute of Steel Construction (AISC) specifications. Afterwards, an experimental study by Broderick and Thomson (2002) involved eight beam-to-column, sub-assemblage, flush end-plate specimens tested under static and dynamic loads. The connection components were selected to ensure a range of failure modes, including both end-plate failure and bolt yielding. The results indicated the appropriateness of this joint type for seismic loading.

The analytical work in this area has focused on the development of more precise design calculations. For example, Mofid *et al.* (2005) calculated the ultimate and yield bending moment

of end-plate moment connections by partitioning the connection's parts into several springs and comparing and validating them experimentally. The authors demonstrated that, among column-web failure modes (e.g. shear yielding, buckling and crippling), shear yielding controlled the connection design. In another study, Lemonis and Gantes (2009) investigated mechanical modelling of the non-linear response of beam-to-column connections using a component method methodology, which was validated experimentally and numerically in terms of stiffness, strength and rotational capacity. The results proved the suitability of the approach and how it can be modified for various beam-to-column joints.

In the same year, Abolmaali *et al.* (2005) introduced several types of finite-element models to consider bi-linear material behaviour, while ignoring the deformation of the column's web and flanges. Specifically, they introduced the 'three-parameter power' model for predicting the bending moment against rotation (M–θ) curve using the Ramberg–Osgood equation (Ramberg and Osgood, 1943). A test matrix of 34 test cases

Figure 3. Extended end-plate moment connection: (a) unstiffened; (b) stiffened

was developed by varying the flush end-plate's geometric variables within its practical range. The FEM model was used to analyse the 34 test cases for M–θ data, which were curve fitted to the Ramberg–Osgood and the 'three-parameter power' model equations to obtain defining parameters. Using regression equations, both models were shown to predict the M–θ plots closely, with the more accurate model being the 'three-parameter power' model. Subsequently, Sumner (2003) studied the influence of a concrete slab and the composite action between the slab and steel girders; in which the presence of slab effects would decrease the separation between the end-plate and the column flange, under monotonic loading. This low rotation resulted from transferring large tensile loads from the slab to the columns, instead of transferring the loads from the bolts and end-plate to the column flange. Furthermore, Shi *et al*. (2007) did some experimental tests on composite joint specimens with flush end-plate connections subjected to cyclic loads. They found that the composite joints with flush

end-plate connections have good moment resistance and rotational capacity under cyclic loading; the presence of the column web stiffener could increase the moment capacity and the initial rotational stiffness of the connection. Additionally, failures of composite joints were observed to be concentrated in the joint zone.

More recently, Ghassemieh *et al*. (2014a) studied the influence of the axial force on the flexural behaviour of the extended, end-plate connection and concluded that the axial forces can alter the failure mode of the connection and, thus, control ultimate moment capacity. Previously, highly innovative work by Shi *et al*. (2008) on the modelling of pre-tensioning forces on an eight-bolt connection under cyclic loading showed new insights in three areas: the pressure distribution caused by pre-tensioning; the friction between the end-plate and the column flange; and the principal stress flow in the connection. Subsequent numerical work by Ghassemieh *et al*. (2014b) on the behaviour of the extended end-plate moment connection subjected to cyclic loading concluded that the end-plate thickness should be chosen so that its ultimate moment capacity is greater than the plastic moment of the beam. If the connection is designed using Fema 350 (Fema, 2000), the plastic hinge is likely to be at a distance of half the beam depth from the end-plate. Recently, numerical work by Zeinoddini-Meimand *et al*. (2014) concluded that end-plate thickness and bolt diameter were effective parameters in characterising the behaviour of flush end-plate connections. If they are appropriately chosen, plastic hinge formation in the connecting beam may be pre-designated. Usually, the beam-to-column joints are subjected to bending moments, and shear and axial forces.

While the axial force is normally ignored, in some structures, the presence of the axial forces in the joints affects directly the structural behaviour. In moment frame or sway frame structures when subjected to significant horizontal loading (seismic or extreme wind), one can expect to have the axial forces developing in the connections. Similarly, in the following circumstances one can expect to have the axial forces in the connections: frames with non-rigid diaphragms; frames with incomplete floors; irregular frames under gravity or horizontal loading; frames during the construction stage; and pitched-roof portal frames (Da Lomba Nunes *et al*., 2007). Nonetheless, despite widespread research on end-plate connections, few studies have explicitly considered the effect of axial loading. De Lima *et al*. (2004) did an experimental study on extended end-plate connections to try to apply the component method philosophy to the combined action of bending moment and axial force. Their results revealed that the presence of an axial force on the beam significantly modifies the joint response. In parallel work, Da Silva *et al*. (2004) conducted experimental and numerical work to investigate the combined action of a bending moment and axial force. To date, this combined loading case has not been considered for flush end-plate
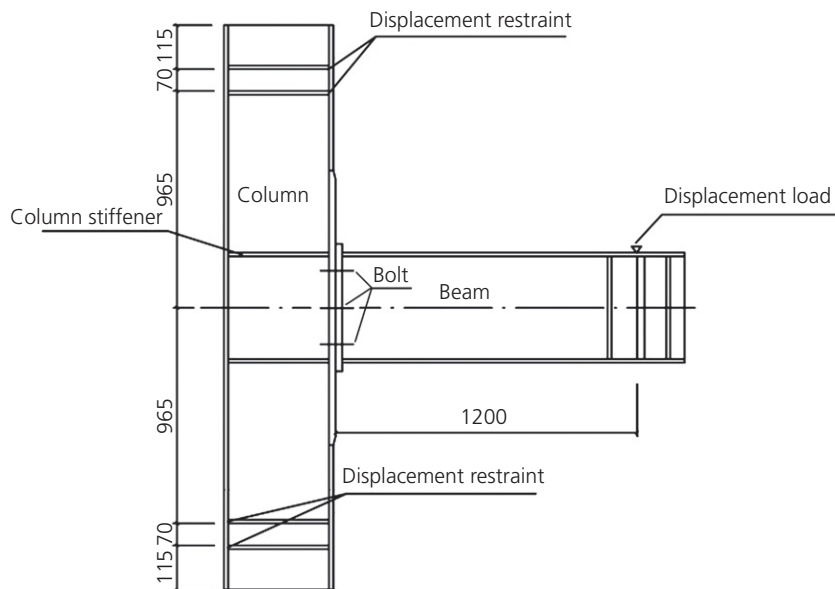
Figure 4. Geometrical dimensions of connection (units in mm) with flush end-plate designed by Shi *et al.* (2008)

connections with respect to their failure modes, which is the topic of the research presented herein.

3. Numerical modelling

This study utilises finite-element modelling to indicate the influence of the axial loading on the behaviour of the flush end-plate moment connections for thin and thick end-plate connections. Specifically considered were large deformations, material non-linearities and accurate contact between parts. The connections were loaded monotonically and cyclically in a combination of axial loading and bending to evaluate the ultimate bending moment, yielding bending moment, initial stiffness and energy dissipation capacity.

To verify the adequacy of the numerical approach, a previously published laboratory experiment was modelled. This was in the form of an unstiffened, flush, end-plate moment connection (SC1) (as per Shi *et al.* (2008), as shown in Figure 4. Tables 1 and 2 present the geometrical specifications of the SC1 specimen.

The top and bottom of the column segment were constrained utilising the hinge supports in the model connection. The vertical displacement was applied at the tip of the beam segment at a distance of 1200 mm from the face of the column flange. Finite-element analysis of the connection was conducted using Abaqus (Abaqus, 2003). All the model components, including beam segment, column, connecting plate and bolts, were modelled using eight-noded, three-dimensional elements (C3D8). In the C3D8 element, each node has three transitional degrees of freedom. After the convergence of the numerical model, the

Table 1. Geometrical dimensions of the beam and column in the connection (Shi *et al.*, 2008)

SC1	Depth: mm	Web thickness: mm	Flange width: mm	Flange thickness: mm
Beam	300	8	200	12
Column	300	8	250	12

final mesh contained 54 363 degrees of freedom with 11 260 elements (Figure 5).

All material properties were based on those reported by Shi *et al.* (2008). The steel for the beam, column and end-plate was assumed to have a yield stress of 391 MPa, an elasticity modulus of 190 GPa and a Poisson ratio of 0·3 and to exhibit bilinear (i.e. elastic–perfectly plastic) behaviour. Material properties of the high-strength bolts are summarised in Table 3. The friction coefficient between the connecting end-plate and column was assumed to be 0·44 and 0·3 for other surfaces. Negative thermal loading was used in Abaqus (Abaqus, 2003) to induce a pre-stress force in the connecting bolts and resulted in a uniform, pre-tension stress in the bolt shanks. The pre-stress force value was set at 680 MPa, equal to 0·55 of bolt ultimate stress, according to JGJ 82-91 (Ministry of Housing and Urban-Rural Development of the People's Republic of China, 1991).

The model of the experimental sample was then subjected to monotonic load and cyclic loading based on the displacement control method according to JGJ 101-96 (Ministry of Housing and Urban-Rural Development of the People's Republic of China, 1996). By comparing the results of the numerical

Table 2. End-plate and bolt dimensions (Shi *et al.*, 2008)

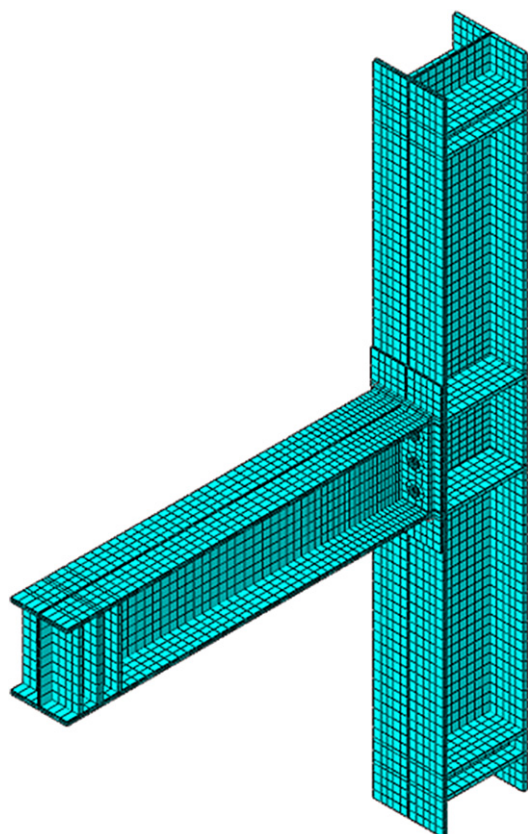| Type of connection	End-plate thickness: mm	Bolt diameter: mm	Number of bolts	Column stiffener: mm
SC1	20	20	6	$276 \times 121 \times 12$

Figure 5. Typical finite-element mesh

Table 3. Tri-linear material behaviour for high-strength bolts

Stress: MPa	0	990	1160	1160
Strain: %	0	0·483	13·6	15

analysis and the experiment, the current finite-element model
was deemed sufficiently realistic for further extrapolation
(Figure 6), as described in the subsequent section.

4. Numerical specimens

Using the ANSI/AISC 358-05 (ANSI/AISC, 2005b) standard,
which follows the AISC design guide series 16 (Murray and
Shoemaker, 2002), two flush end-plate moment connections
were designed so that one specimen was expected to have thick
end-plate moment connection behaviour (EP1) and the other
thin end-plate moment connection behaviour (EP2), as shown
in Figure 7. The connection detailing and geometry matched
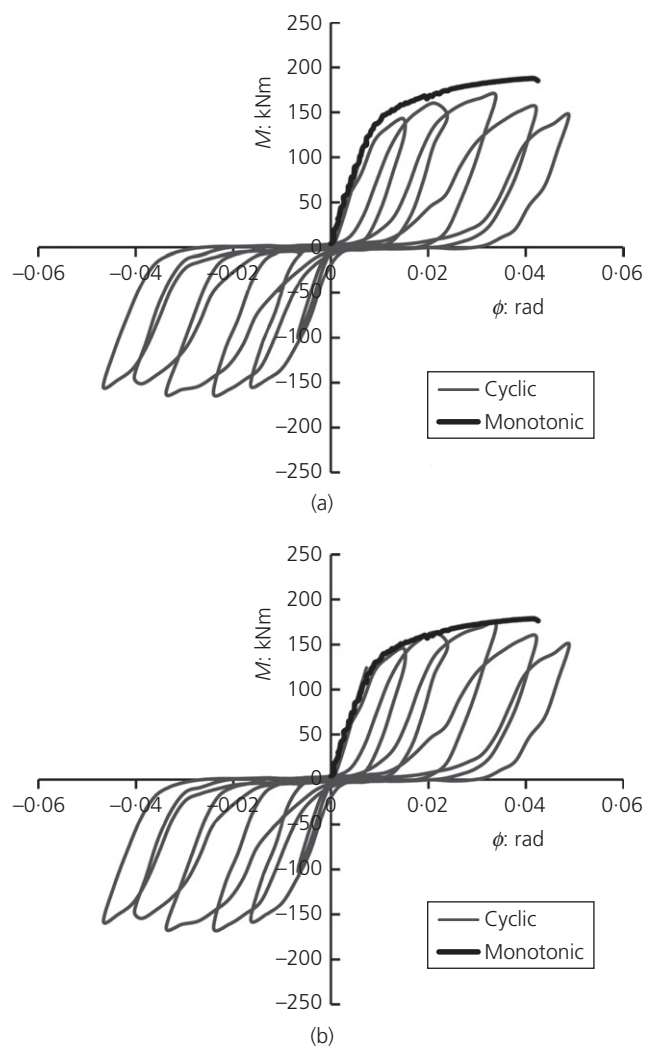those tested by Shi *et al.* (2008), except for the end-plate

Figure 6. Validation of the proposed numerical model:
(a) moment plotted against rotation curve for the sample tested
by Shi *et al*. (2008); (b) moment plotted against rotation curve of
the finite-element model

thickness, bolt sizing and bolt locations. Tables 4 and 5 sum-
marise the geometrical dimensions of the components of these
two connections.

4.1 Flexural capacity of EP1 and EP2 connections
When an end-plate is thick, the prying force is excluded from
the calculations, because the end-plate deformation is low and
can, therefore, be considered as negligible. Hence, the bolt
failure mode is expected to be of the fracture mechanism type,
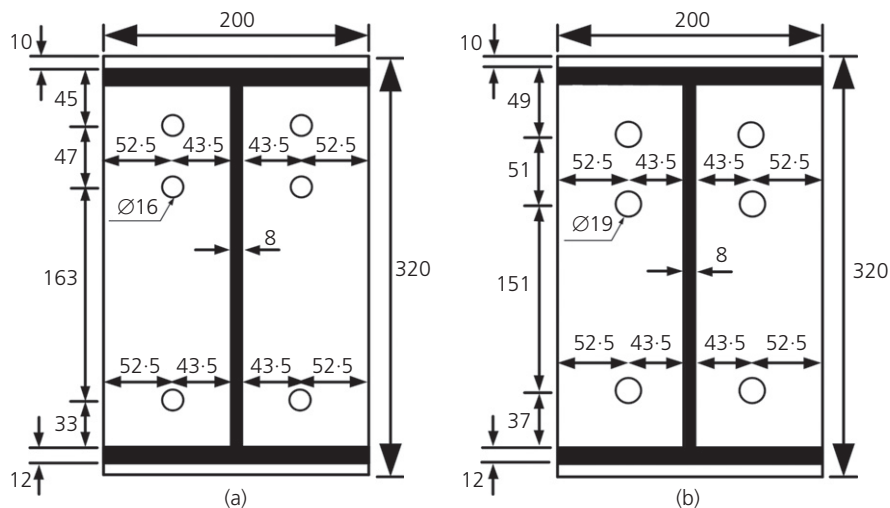and the end-plate is expected to remain entirely elastic until

Figure 7. Flush end-plate connection dimensions (units in mm): (a) EP1 thick specimen; (b) EP2 thin specimen

failure. Table 6 gives the ultimate moment capacity of the connections. In the table, $M_{u\text{-}FE}$ is the ultimate moment capacity of the connection obtained from the finite-element model; M_{np} is the nominal moment capacity of the connection according to AISC design guide series 16 (Murray and Shoemaker, 2002) based on the tensile bolt fracture, without considering the prying force; and M_{pl} is the nominal moment capacity of the connection based on end-plate yielding, as calculated from AISC design guide series 16 (Murray and Shoemaker, 2002).

Since the EP1 end-plate was thick, the value of plastic bending moment of the end-plate was (as expected) higher than the value of the ultimate bending moment of the bolts without the prying force (Table 6). For this EP2 model, the flexural capacity of the connection was calculated (Table 6), and no significant difference was seen between the plastic moment of the end-plate ($M_{pl} = 253·16$ kNm) and the moment produced by the bolts without the prying force ($M_{np} = 246·44$ kNm).

The results obtained from the EP2 finite-element analysis showed that the ultimate strength of the connection ($M_{u\text{-}FE}$)

was smaller than both the ultimate bending moment of the bolt without the prying force and the ultimate plastic moment of the end-plate. This was due to the presence of the prying force, which formed a moment in the opposite direction of the applied moment and, therefore, reduced the bending capacity of the connection ($M_{u\text{-}FE} < M_{np}$).

5. Behaviour of the thick, flush end-plate connections with axial loading

In this section, the effects of axial load on the behaviour of the EP1 thick, flush end-plate connection were investigated. Parameters such as flexural capacity, failure mode, initial stiffness of connection, plastic strain and stress of the bolts were examined in detail. Loading was conducted in three main areas: (*a*) formation of pre-tension in the bolts; (*b*) application of axial force, which was increased linearly from zero to a percentage of the yield force of the beam section; and (*c*) application of flexural loading to the connection (i.e. after application of axial force was completed).

To better understand the behaviour of these connections under the influence of the axial force and the bending moment simultaneously, the interaction diagram of the axial force plotted against the bending moment of the connection is drawn in Figure 8. The interaction diagram was constructed for the EP1 model by varying the axial force from the maximum compressive force (equal to almost 100% of the beam yield strength) up to the maximum tensile force (equal to about 38% of the beam yield strength). Figure 8 illustrates the variation of the

Table 4. Beam and column section properties of the connection

	Depth: mm	Web thickness: mm	Flange width: mm	Flange thickness: mm
Beam	300	8	200	12
Column	300	12	250	18

Table 5. Geometrical properties of the flush end-plate connections

Connection type	End-plate thicknes: mm	Bolt diameter: mm	Number of bolts	Column stiffener: mm
EP1	30	16	6	264 × 119 × 12
EP2	19	19	6	264 × 119 × 12

6

Table 6. Ultimate moment connections

Connection	$M_{u\text{-FE}}$: kNm	M_{pl}: kNm	M_{np}: kNm	$\dfrac{M_{pl}}{M_{u-FE}}$	$\dfrac{M_{np}}{M_{u-FE}}$
EP1	199	658·23	172·77	3·3	0·868
EP2	211·5	253·16	246·44	1·197	1·165

axial force with respect to the moment capacity of the connection. The moment ratio (R) was calculated by dividing the ultimate moment obtained from the analysis with inclusion of the axial force by the ultimate moment of the connection without the axial force. In this figure, P is the axial stress applied to the beam section, and $F_{y\text{-beam}}$ is the yield stress of the beam section.

Three main zones were observed in the interaction diagram. In zone 1, the connection failure was controlled by the tensile capacity of the bolts. Based on the interaction curve, the moment ratio increased with diminishing axial tensile force. Consequently, the flexural capacity of the connection increased. Thus for point 1 in this zone, corresponding to $P/F_{y\text{-beam}}$ equal to 0·38, there was no bending moment capacity. In fact at this point, the ultimate tensile capacity (P) was obtained from the tensile capacity of the bolts where part of it was lessened by the presence of the pre-stress force in the bolts. In zone 2, the bending capacity of the connection increased with more axial force. This increase continued up to $P/F_{y\text{-beam}} = -0·3$ (point 2). The connection failure was controlled by the bolts in this zone. In zone 3, unlike zone 2, bending capacity of the connection was reduced with an increase in the axial compressive force. This was due to buckling of the beam flanges and gives rise to the conclusion that the failure mode of the connection changed from that of a bolt failure to buckling of the beam's compressive flange. The axial force increased in this zone, until the bending capacity of the
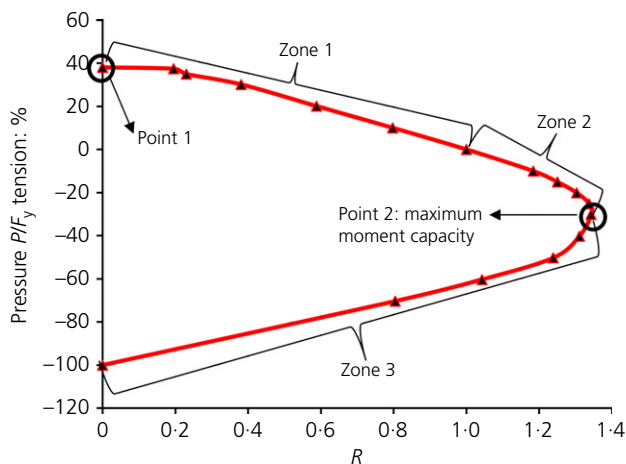
connection was lost completely. This occurred when the stress in the beam section approached its yield stress.

5.1 Stresses and plastic strains in the bolts

The stress in the top row bolts of the EP1 models is shown in Figure 9. The initial flat portions can be ascribed to the pre-tensioning approximate to tensile axial stress of 10% $F_{y\text{-beam}}$ (see specimen EP1+10). The pre-tensioning effects dissipated with additional tensile axial loading. In most cases, the maximum stress in the top row of bolts was 1160 MPa, which represented failure of the connection. However, when the compressive axial stress exceeded 30% $F_{y\text{-beam}}$, the failure was in compressive-flange buckling (zone 3). As the axial force increased, the buckling of the compressive flange occurred at a lower bending moment, and the bolt stress value did not increase. Figure 10 illustrates the Von-Mises stress in the middle bolts with respect to the applied moments. As the behaviour of the connection is the thick end-plate type, the behaviours of the bolts located in the first and the second row were nearly identical.

Plastic strain levels in the bolts of the connection under axial force can be indicative of the effects of axial force on bolt plasticity. According to Figure 11, plastic strain behaviour of the first row of bolts indicates that these bolts exhibited plastic behaviour faster under axial tension stress of 30% $F_{y\text{-beam}}$, compared to the other loading cases. Additionally, maximum plastic strain was reduced severely at the end of loading under compressive axial stresses higher than 30% $F_{y\text{-beam}}$.

5.2 Connection stiffness

Figure 12 shows the bending moment plotted against rotation for different samples of EP1 connections under various axial loadings. Maximum rotation values were checked under the compressive stress of 15% $F_{y\text{-beam}}$. At the axial tensile stresses equal to 30% $F_{y\text{-beam}}$, 20% $F_{y\text{-beam}}$ and 10% $F_{y\text{-beam}}$, the rotation values were approximately equal to EP1 (i.e. numerical

Figure 8. Axial force ratio plotted against bending moment interaction ratio for EP1 (the positive sign indicates tensile axial force, and negative sign depicts compressive axial force)
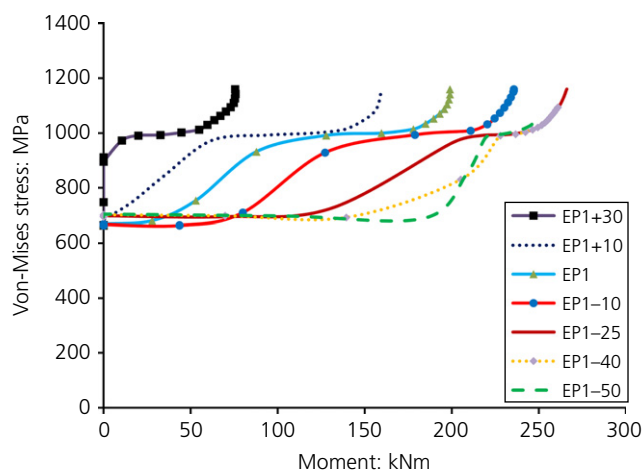

Figure 9. Von-Mises stress plotted against bending moment in the upper bolts of EP1 connection
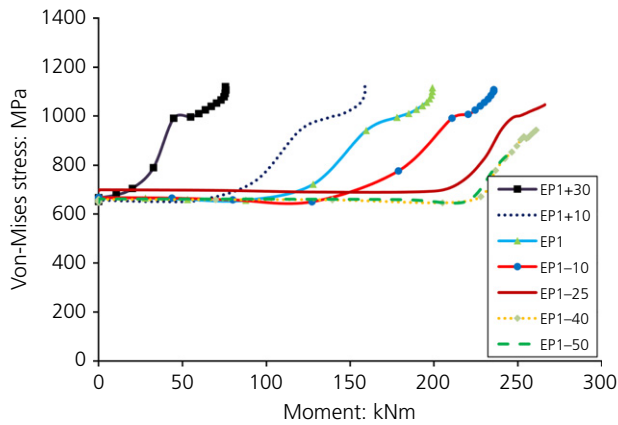
Figure 10. Von-Mises stress plotted against bending moment in
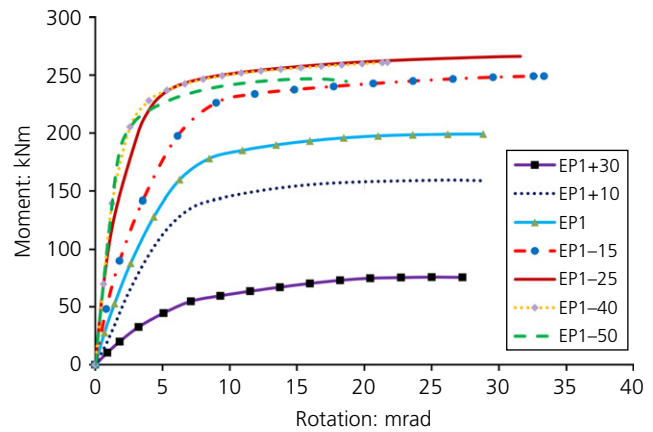the middle bolts of EP1 connection

Figure 12. Moment plotted against rotation curve of EP1
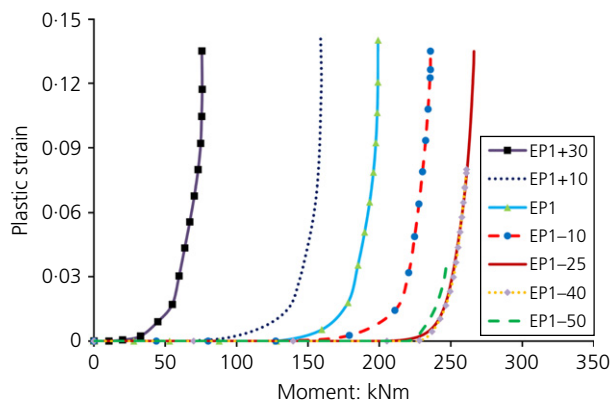connection with different axial forces

Figure 11. Plastic strain plotted against bending moment in the
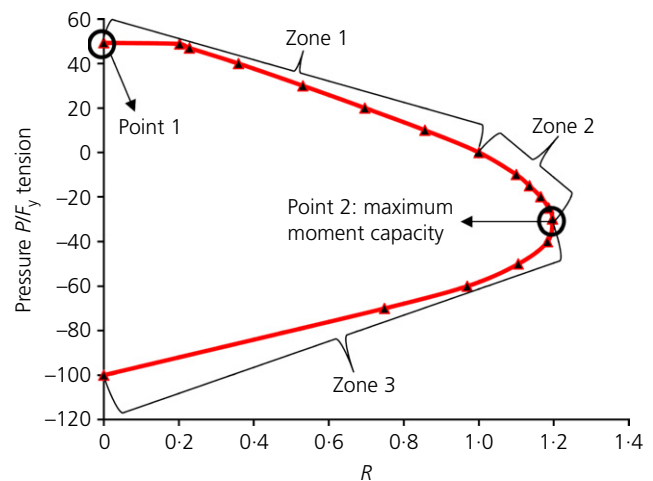upper bolts of EP1 connection

Figure 13. Axial force ratio plotted against bending moment
ratio (EP2)

specimen without axial force). When the compressive axial stress exceeded 30% $F_{\text{y-beam}}$, the connection rotation reduced significantly. This decline indicated that the connection failure changed from bolt rupturing to compressive flange buckling. According to Figure 12, the initial stiffness of the connection decreased with the application of greater axial tensile force and increased with greater compressive axial force (as would be expected); the minimum and maximum initial stiffness of the connections were observed within the EP1+30 and EP1−50 cases, respectively. The sample EP1+30 was less stiff than the others since its axial tensile force effectively removed the pre-tensioning effect of the bolts entirely and, thus, caused a decrease of the connection stiffness.

6. Behaviour of the thin, flush end-plate connections including the axial loading

In this section the effects of the axial load on behaviour of the EP2 (thin, flush end-plate moment) connection were investigated. The bending moment plotted against axial force inter-action diagram of Figure 13 was divided into three zones. In

zone 1, the bending moment of the connection increased when tensile axial force decreased. The failure of the tensile bolts and the formation of a plastic hinge on the end-plate was the dominant failure mode occurring around the tensile flange of the beam and adjacent to the first row bolts. At the beginning of this zone (point 1), the connection bending moment dissipated, because of the applied tension axial force, and the connection failed due to the yielding of the bolts. In zone 2, the bending moment of the connection increased with more compressive axial force. At the end of this zone, the moment of the connection reached its maximum value under axial stress of −30% $F_{\text{y-beam}}$ at point 2. Similar to zone 1, the connection failed due to the failure of the bolts and the end-plate yielded near the tensile flange and around the first row of the bolts. In zone 3, the moment of connection reduced when the compressive axial force increased. This denoted the change in failure mode from bolt rupture mode to compressive beam flange

8

buckling. The end point of zone 3 shows that the moment resistance of the connection decreased under axial compressive stress to -100% $F_{\text{y-beam}}$.

6.1 Stresses and plastic strains in the bolts

Figure 14 shows the stress changes in the first row bolts plotted against the moment in the connection during loading. The stress of the first row of bolts reached a maximum value of 1160 MPa at the end of the loading, except when with compressive axial stresses exceeded 30% $F_{\text{y-beam}}$ where the first row bolts did not fracture, and the failure mode was local buckling of the beam flange. This change in failure mode prevented the bolts from reaching their ultimate strength.

Figure 15 shows the change in the stress value of the second row bolts plotted against the moment connection. According to this figure, the stress did not reach its ultimate value as the end-plate was thin, and the plastic hinge formed on the
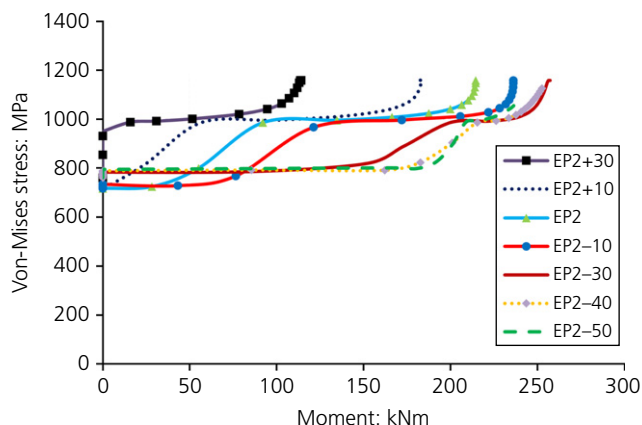
end-plate near the first row of bolts. Furthermore, the plate did not remain flat, which caused the strain in the second row bolts to diverge in behaviour from the first row bolts' strain. The plastic strain was assessed in the bolts to detect the effects of axial force on bolt plasticity. According to Figure 16, the ultimate plastic strain of the first row bolts was noticeably reduced under compressive axial stresses higher than 30% $F_{\text{y-beam}}$.

6.2 Connection stiffness

According to Figure 17, the stiffness of the connection increased with decreasing tensile axial forces and/or increasing compressive axial forces; also as illustrated in Figure 17, the bolt stress plotted against moment diagram, the horizontal part of the curve dropped with an increase in the tensile axial force.

7. Studying the cyclic behaviour of connections with the axial load

In this section, the behaviour of the above two numerical model connections (i.e. 'EP1-cyclic' and 'EP2-cyclic') were

Figure 14. Von-Mises stress plotted against bending moment in the upper bolts of EP2 connection

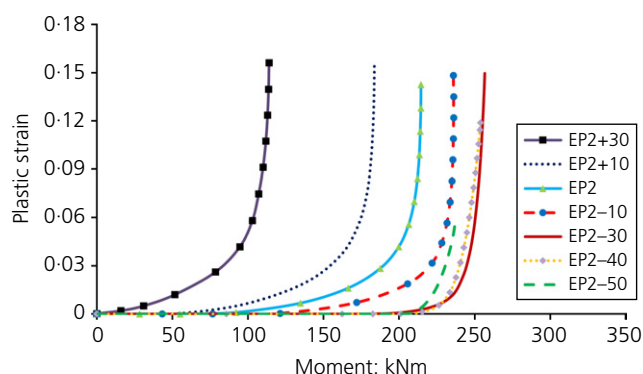**Figure 16.** Plastic strain plotted against bending moment in the upper bolts of EP2 connection

Figure 15. Von-Mises stress plotted against bending moment in the middle bolts of EP2 connection
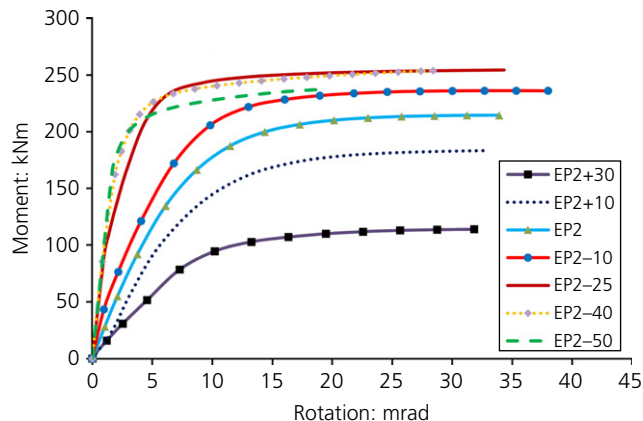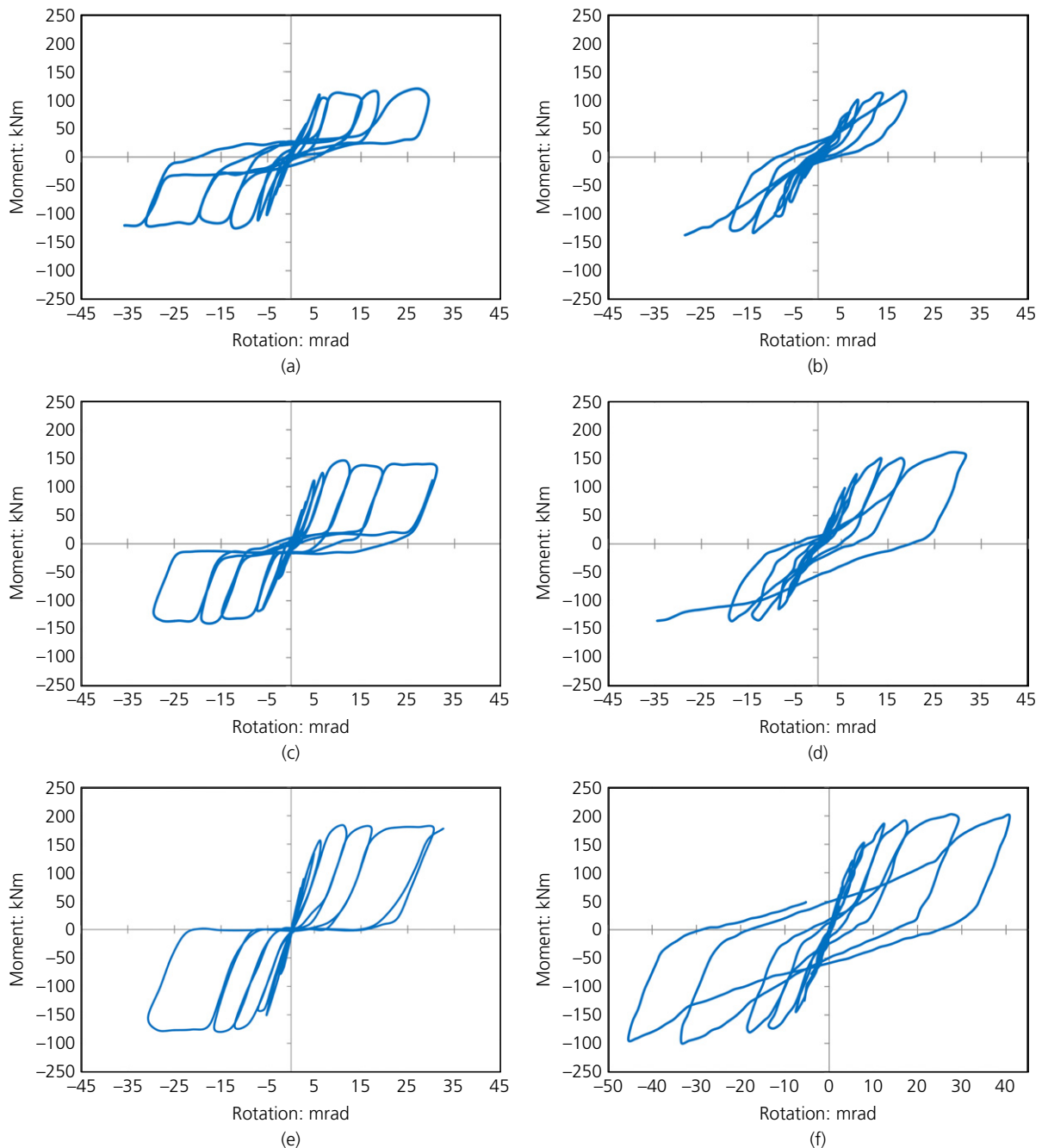

Figure 17. Moment plotted against rotation in EP2 connection with different axial forces

investigated under reversed cyclic loading in accordance with the SAC loading protocol (SAC representing a joint venture between the Sturctural Engineering Association of California, the Applied Technology Council and the California Universities for Research into Earthquake Engineering (SAC Joint Venture, 1997)) along with a constant axial load. The moment plotted against rotation curves for several samples

subjected to axial force ranging from 15% of the tensile capacity of the beam to 20% of the compressive capacity of the beam are provided in Figure 18.

From the curves presented in Figures 18(a)–18(l), as expected, the value of the ultimate bending moment, yielding bending moment and the initial stiffness all increased with higher levels

Figure 18. Moment plotted against rotation hysteresis curves for different sample model connections: (a) EP1-cyclic+15;
(b) EP2-cyclic+15; (c) EP1-cyclic+10; (d) EP2-cyclic+10; (e) EP1-cyclic; (f) EP2-cyclic; (g) EP1-cyclic−10; (h) EP2-cyclic−10; (i) EP1-cyclic−15;
(j) EP2-cyclic−15; (k) EP1-cyclic−20; (l) EP2-cyclic−20 (continued on next page)
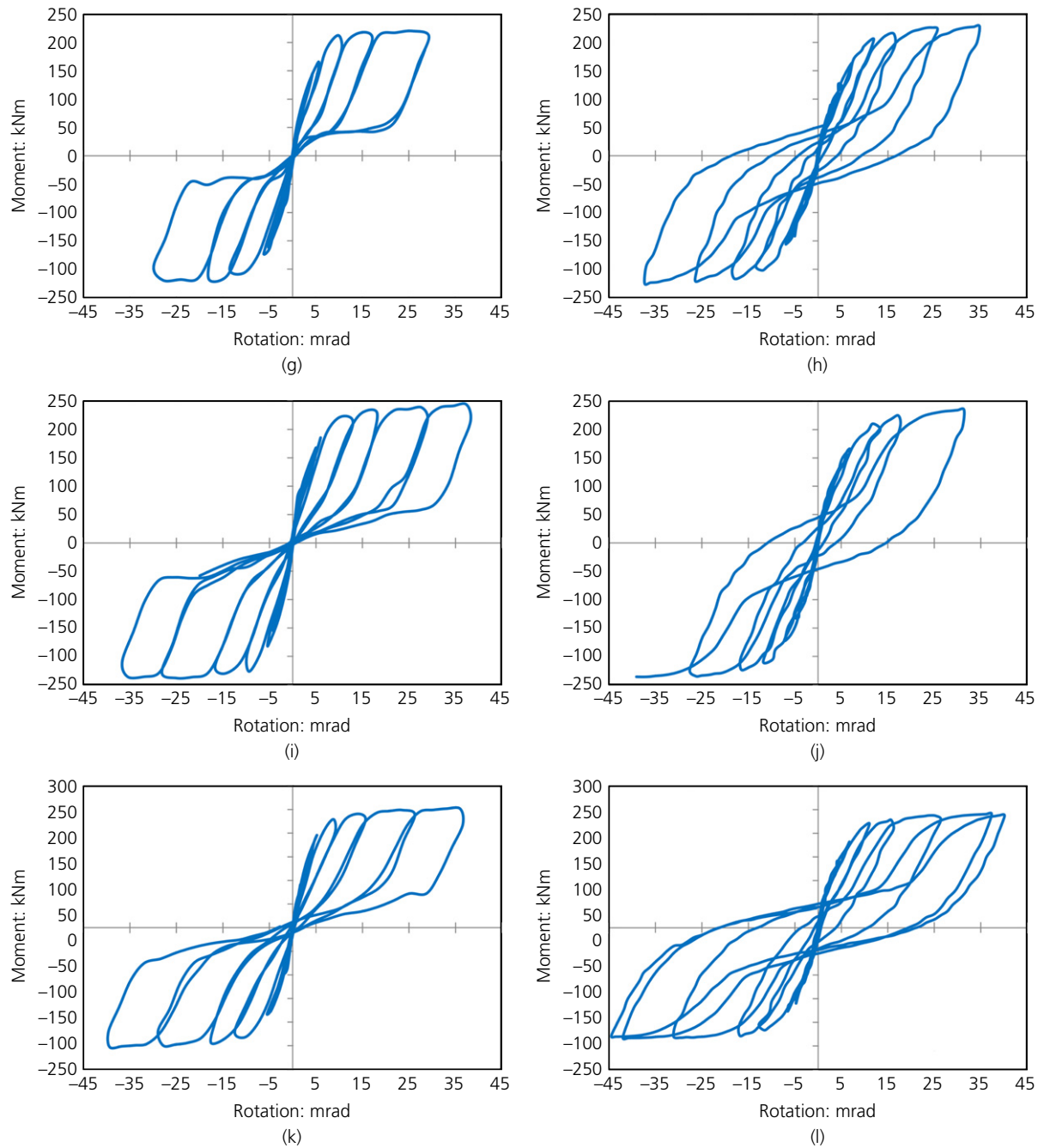
Figure 18. Continued

of the compressive axial load and reduced when tensile axial load was applied. Similarly, the energy dissipation of the sample connections increased in the presence of the compressive axial load and diminished in the presence of the tensile axial force. Also as expected, the connection with the thin end-plate (EP2) showed higher ductility than that of the thick end-plate (EP1) owing to the changes in the thickness of the end-plate and the bolt diameter.

8. Conclusions

In this study, the flexural behaviour of a flush end-plate moment connection subjected to a combined axial force and bending moment was investigated using a non-linear, finite-element method of analysis. The behaviour of such connections subjected to different loading conditions, such as monotonic and cyclic loading, was examined. From the findings of this study, the following conclusions were drawn.

- The general shape of the interaction curve was independent of the connections' dimensions.
- The maximum moment capacity was seen on the compressive axial force equal to nearly 30% of the beam section yield stress (Figures 8 and 13).
- The thin end-plate connection had higher ductility than the thick end-plate connection owing to the thickness of the end-plate and the diameter of connecting bolts, which caused the bolts, end-plate and beam to contribute to the connection ductility (Figures 12 and 17).
- The values of ultimate bending moment, yielding moment, initial stiffness and energy dissipation of connection increased with higher levels of compressive axial load and decreased under tensile axial loads.

REFERENCES

Abaqus (2003) *Abaqus User's Manual, Version 6.4*. Abaqus Inc., Providence, RI, USA.

Abolmaali A, Matthys JH, Farooqi M and Choi Y (2005) Development of moment–rotation model equations for flush end-plate connections. *Journal of Constructional Steel Research* **61(12)**: 1595–1612.

ANSI/AISC (American National Standard Institute/American Institute of Steel Construction) (2005a) *ANSI/AISC 341-05, Seismic Provisions for Structural Steel Buildings*. American Institute of Steel Construction, Chicago, IL, USA.

ANSI/AISC (2005b) *ANSI/AISC 358-05, Prequalified Connections for Special and Intermediate Steel Moment Frames for Seismic Applications*. American Institute of Steel Construction, Chicago, IL, USA.

Boorse MR (1999) *Evaluation of the Inelastic Rotation Capability of Flush End-Plate Moment Connections*. Department of Civil Engineering, Virginia Polytechnic Institute and State University, Blacksburg, VA, USA.

Bose B, Wang ZM and Sarkar S (1997) Finite-element analysis of unstiffened flush end-plate bolted joints. *Journal of Structural Engineering* **123(12)**: 1614–1621.

Broderick BM and Thomson AW (2002) The response of flush end-plate joints under earthquake loading. *Journal of Constructional Steel Research* **58(9)**: 1161–1175.

Da Lomba Nunes PC, De Lima LRO, Da Silva JGS, Da S. Vellasco PCG and De Andrade SAL (2007) Parametrical analysis of extended endplate semi-rigid joints subjected to bending moment and axial force. *Latin American Journal of Solids and Structures* **4(1)**: 39–59.

Da Silva LS, De Lima LR, Da S. Vellasco PCG and De Andrade SA (2004) Behaviour of flush end-plate beam-to-column joints under bending and axial force. *Steel and Composite Structures* **4(2)**: 77–94.

De Lima LRO, Da Silva LS, Da S. Vellasco PCG and De Andrade SAL (2004) Experimental evaluation of extended endplate beam-to-column joints subjected to bending and axial force. *Engineering Structures* **26(10)**: 1333–1347.

Fema (Federal Emergency Management Agency) (2000) *FEMA-350 – Recommended Seismic Design Criteria for New Steel Moment-Frame Buildings (Prepared by SAC Joint Venture)*. Federal Emergency Management Agency, Washington, DC, USA.

Ghassemieh M, Shamim I and Gholampour AA (2014a) Influence of the axial force on the behavior of end-plate moment connections. *Structural Engineering and Mechanics* **49(1)**: 23–40.

Ghassemieh M, Jalalpour M and Gholampour AA (2014b) Numerical evaluation of the extended end-plate moment connection subjected to cyclic loading. *Current Advances in Civil Engineering* **2(1)**: 35–43.

Lemonis ME and Gantes CJ (2009) Mechanical modeling of the nonlinear response of beam-to-column joints. *Journal of Constructional Steel Research* **65(4)**: 879–890.

Ministry of Housing and Urban-Rural Development of the People's Republic of China (1991) JGJ 82-91: Specification for design, construction and acceptance of high strength bolt connections in steel structures. China Architecture and Building Press, Beijing, China.

Ministry of Housing and Urban-Rural Development of the People's Republic of China (1996) JGJ 101-96: Specification for testing methods for earthquake-resistant buildings. China Architecture and Building Press, Beijing, China.

Mofid M, Mohammadi MRS and McCabe SL (2005) Analytical approach on end-plate connection: ultimate and yielding moment. *Journal of Structural Engineering* **131(3)**: 449–456.

Murray TM and Shoemaker WL (2002) *AISC Design Guide Series 16 (Flush and Extended Multiple-Row Moment End-Plate Connections)*. American Institute of Steel Construction, Chicago, IL, USA.

Ramberg W and Osgood WR (1943) *Description of Stress–Strain Curves by Three Parameters*. National Advisory Committee for Aeronautics, Washington, DC, USA, Technical Note No. 902.

SAC Joint Venture (1997) *Protocol for Fabrication, Inspection, Testing and Documentation of Beam–Column Connection Tests and Other Experimental Specimens*. SAC Steel Project, SAC Joint Venture, Sacramento, CA, USA, Report No. SAC/BD-97.

Shi WL, Li GQ, Ye ZM and Xiao RY (2007) Cyclic loading tests on composite joints with flush end plate connections. *International Journal of Steel Structures* **7(2)**: 119–128.

Shi G, Shi Y, Wang Y and Bradford MA (2008) Numerical simulation of steel pretensioned bolted end-plate connections of different types and details. *Engineering Structures* **30(10)**: 2677–2686.

Sumner EA (2003) *Unified Design of Extended End-Plate Moment Connections Subject to Cyclic Loading*. PhD dissertation, Department of Civil Engineering, Virginia Polytechnic Institute and State University, Blacksburg, VA, USA.

Zeinoddini-Meimand V, Ghassemieh M and Kiani M (2014) Finite element analysis of flush end-plate moment connections under cyclic loading. *International Journal of Civil, Architectural Science and Engineering* **8(1)**: 96–104.

How can you contribute?

To discuss this paper, please email up to 500 words to the editor at journals@ice.org.uk. Your contribution will be forwarded to the author(s) for a reply and, if considered appropriate by the editorial board, it will be published as discussion in a future issue of the journal.

Proceedings journals rely entirely on contributions from the civil engineering profession (and allied disciplines). Information about how to submit your paper online is available at www.icevirtuallibrary.com/page/authors, where you will also find detailed author guidelines.